Enhancements of FRL08 : metrological connection between simulation/experiment and utilization of AI tools for coincidence matrix analysis

Authors : **H.-D. Lenouvel**[1], H. Paradis[1]
Co-authors : A. de Vismes Ott[1], P. Gross[1], S. Topin[1,2]

[1] CEA, DAM, DIF, F-91297 Arpajon, France
[2] CNAM, Analyse Chimique et Bioanalyse, EPN-7, 292 rue Saint Martin, 75003 Paris, France

09 september 2025

H.-D. Lenouvel, H. Paradis, A. de Vismes Ott, P. Gross, S. Topin

From context to modeling : systems and methods

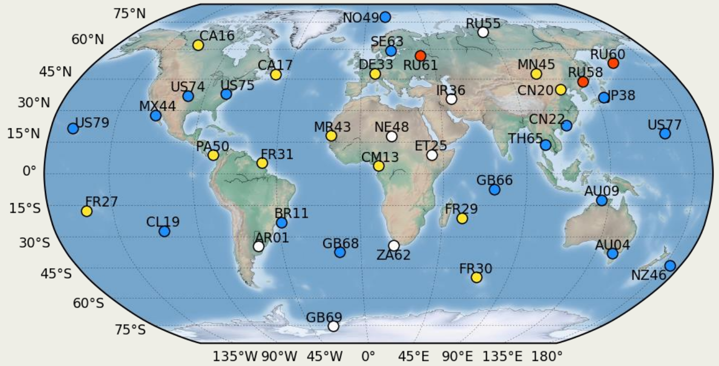

Enhancements of FRL08 : metrological connection between simulation/experimental and utilization of AI tools for coincidence matrix analysis

H.-D. Lenouvel, H. Paradis, A. de Vismes Ott, P. Gross, S. Topin

O3.2-267

Radionuclide technology : context and stakes

- Resources deployed by the CEA as part of the CTBT framework:
  - Stations: SPALAX and SPALAX-NG [1]
  - **Certified Laboratory: FRL08 (Gamma³)** [2]
  - National Data Center (NDC)

- Research for radionuclide measurements:
  - **Coincidence measurements** (with the SPALAX-NG and Gamma³)
  - **Data analysis** : AI and spectral unmixing methods (P3.2-263)

Fig 1. SPALAX-NG

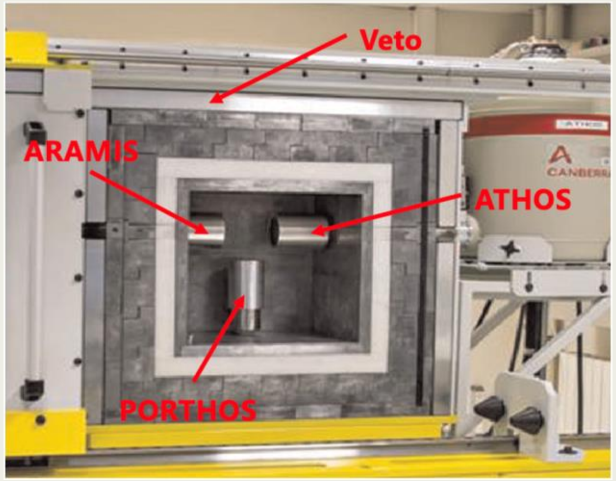

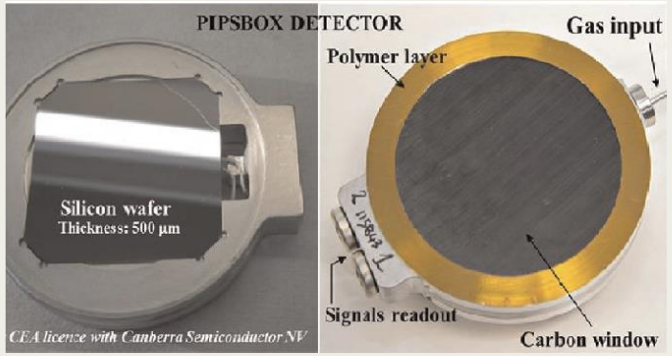

Fig 2. Gamma³ (left) & PIPSBox (right)

[1] S. Topin et al., J. Environ. Radioact. 225 (2020) 106442
[2] A. Cagniant et al., Applied Radiation and Isotopes 98 (2015)

H.-D. Lenouvel, H. Paradis, A. de Vismes Ott, P. Gross, S. Topin

Model creation with MCNP

- Modeling from:
  - Technical drawings provided by the manufacturer
  - Radiographies of detectors

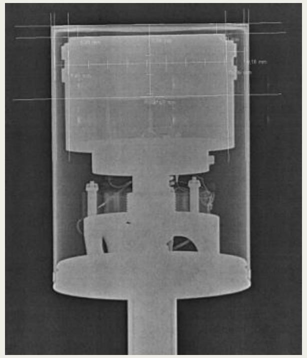

Fig 3. Radiography of a HPGe detector (BEGe5030P)

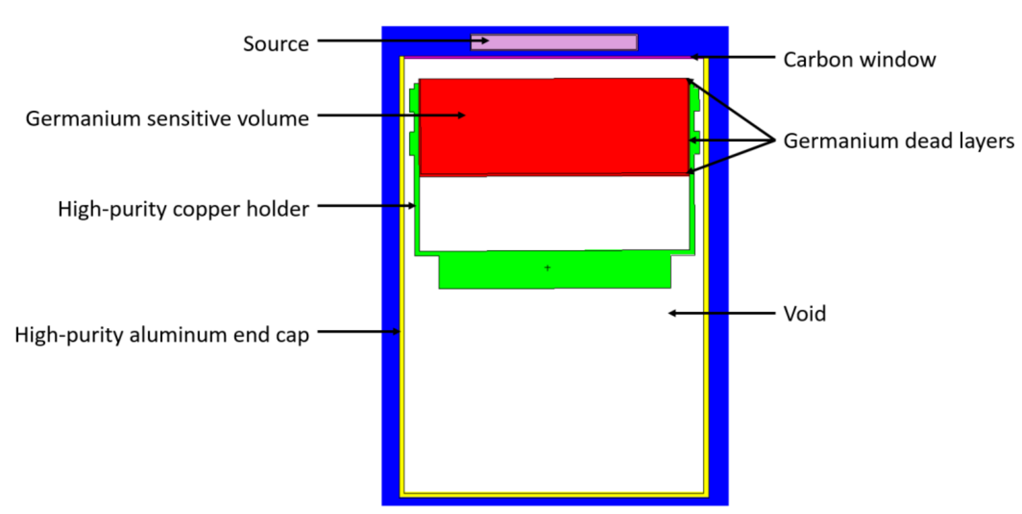

Fig 4. Display of a cross-sectional view of a detector modeled under MCNP.

- Standard sources:
  - <u>Energy range covered:</u> [22 - 2505 keV]
  - <u>Geometries:</u>
    - compressed or uncompressed particle filters (diameter of 110 mm)
    - volumetric geometries (from 20 mL to 500 mL)

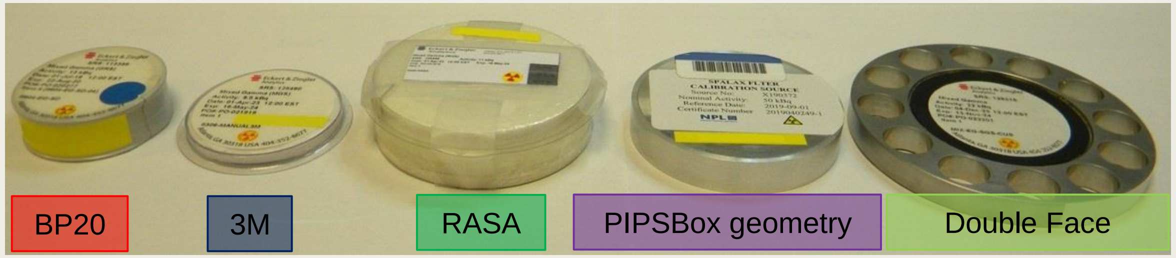

Fig 5. Common sources geometry used by the laboratory

➔ **Use of sources of different sizes and compositions to provide a general calibration**

Enhancements of FRL08 : metrological connection between simulation/experimental and utilization of AI tools for coincidence matrix analysis

H.-D. Lenouvel, H. Paradis, A. de Vismes Ott, P. Gross, S. Topin

Validation of models

- Detection efficiency: $\varepsilon = (\text{number of particles detected})/(\text{number of particles emitted})$
- Validation of the digital model:

1° Modeling of detectors

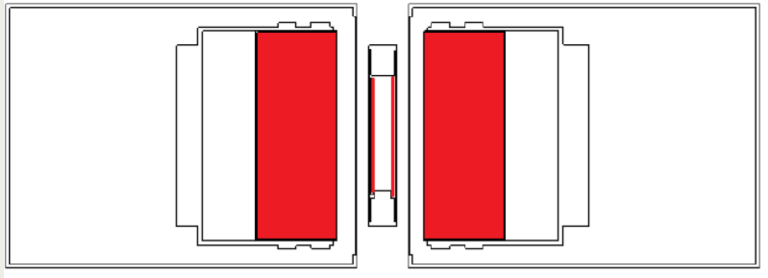

Fig 6. Modeling of the configuration (ATHOS + ARAMIS) & PIPSBox

2° Optimization:
Mean ratio = $\left(\frac{\varepsilon_{EXP}}{\varepsilon_{MCNP}}\right) \approx 1$

3° Validation of models

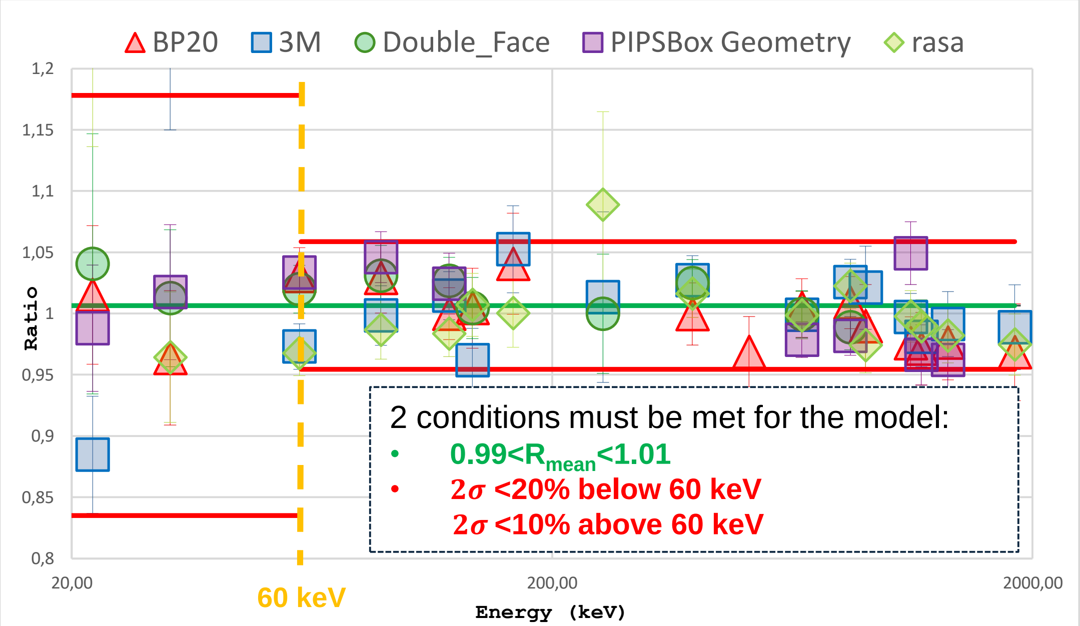

Fig 7. Detection efficiency ratio (EXP/MCNP) versus energy

- Parameters to optimize:
  - Thickness of materials (dead layers, carbon window…)
  - Position of the source relative to the crystal detector
  - Crystal size

$$A = N_{net} * \frac{1}{\boldsymbol{\varepsilon}} * \frac{1}{I} * \frac{1}{T} * \prod_i C_i$$

➔ **Model validation enables simulation for calculating new detection efficiencies**

ε from A. Berlizov, MCNP-CP Upgrade Patch Version 3.2, Institute for Nuclear Research National Academy of Sciences of Ukraine, 2012

H.-D. Lenouvel, H. Paradis, A. de Vismes Ott, P. Gross, S. Topin

Quantification through coincidence measurements

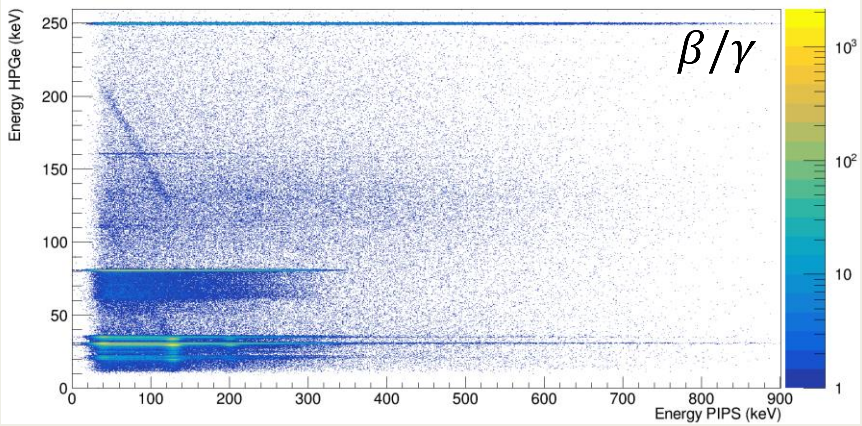

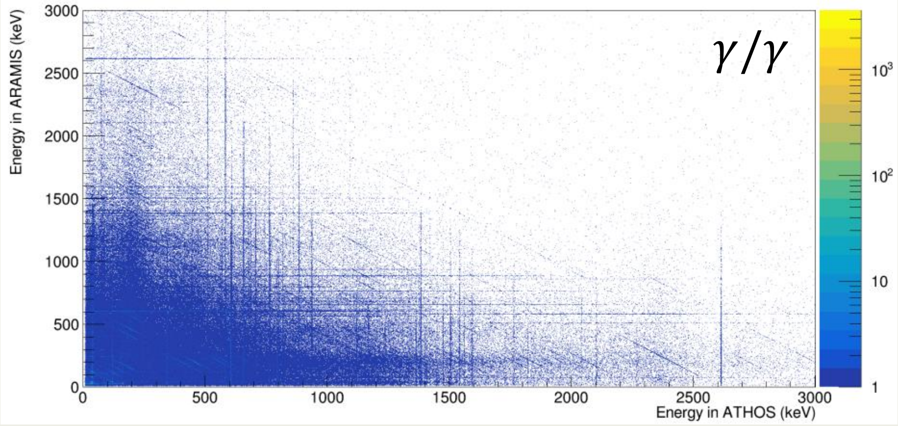

H.-D. Lenouvel, H. Paradis, A. de Vismes Ott, P. Gross, S. Topin

Validation of the method on a gaseous sample

- Measurement:
  - (ATHOS+ARAMIS)&PIPSBox
  - Duration: 57600 s

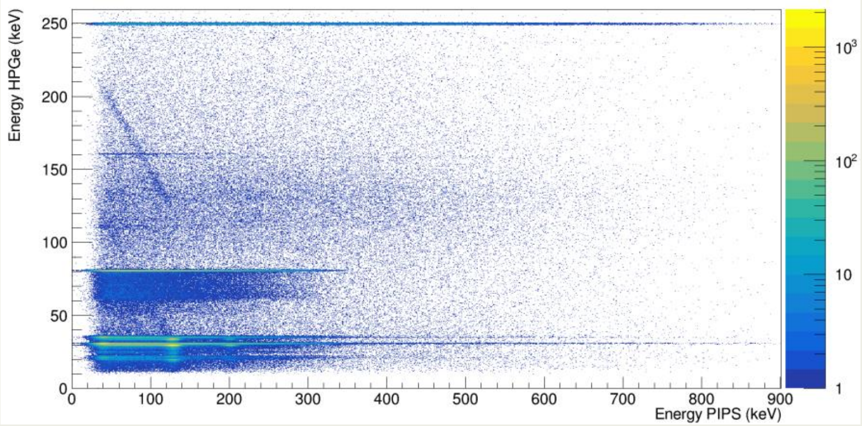

Fig 8. β/γ **matrix obtained from the measurement**

- Efficiency calculation:
  - MCNP-CP

Tab 1. β/γ **detection efficiencies for the 4 radioxenon isotopes**

RXe	β/γ coincidence spectrometry
^{131m}Xe	0.16 ± 0.02
^{133}Xe	0.20 ± 0.02
^{133m}Xe	0.147 ± 0.023
^{135}Xe	0.176 ± 0.016

- Analysis:

Tab 2. Comparison between reference activities and measured activities

RXe	A_{ref} (Bq)	$U(A_{ref})$ k=2 (Bq)	A_{meas} (Bq)	$U(A_{meas})$ k=2 (Bq)	Deviation (%)	E_n score
^{131m}Xe	94	10	84	13	-10.6	-0.60
^{133}Xe	204	23	205	19	0.8	0.06
^{133m}Xe	10.2	1.1	9.1	1.4	-11.3	-0.63
^{135}Xe	217	22	226	21	4.0	0.29

➔ **Validation for γ-ray spectrometry and for β/γ coincidence spectrometry. Very good agreement with reference values.**

➔ **H.-D. Lenouvel, et al., *Measurement of radioxenon isotopes for nuclear explosion detection using coincident β/γ detector calibrated by simulation*, ARI. DOI: ARI 111886**

H.-D. Lenouvel, H. Paradis, A. de Vismes Ott, P. Gross, S. Topin

Benefits of using γ/γ coincidence detection (example with ^{134}Cs)

- Identification of ^{134}Cs using coincidences:

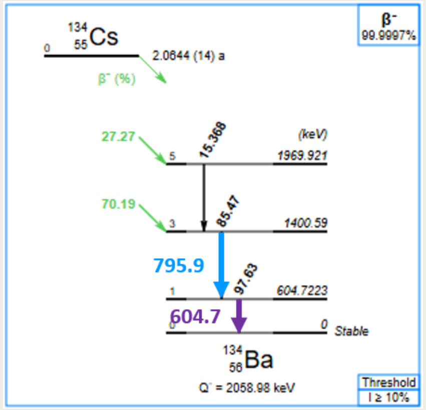

Fig 9. Decay scheme of ^{134}Cs

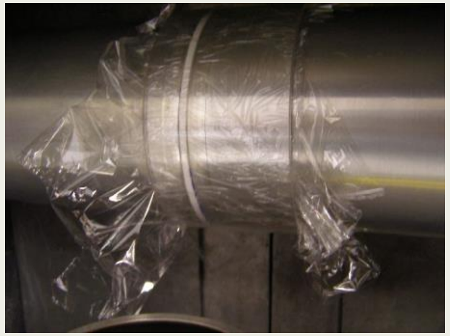

Fig 10. Particulate filter placed between two HPGe detectors with expected coincidence matrix signatures

- Measurement of a fresh fission products sample from CTBTO:
  - Classic γ-ray spectrometry: complex spectra (~300 peaks)
  - Coincidence spectrometry: characteristic signatures

SNR : Signal-to-Noise Ratio

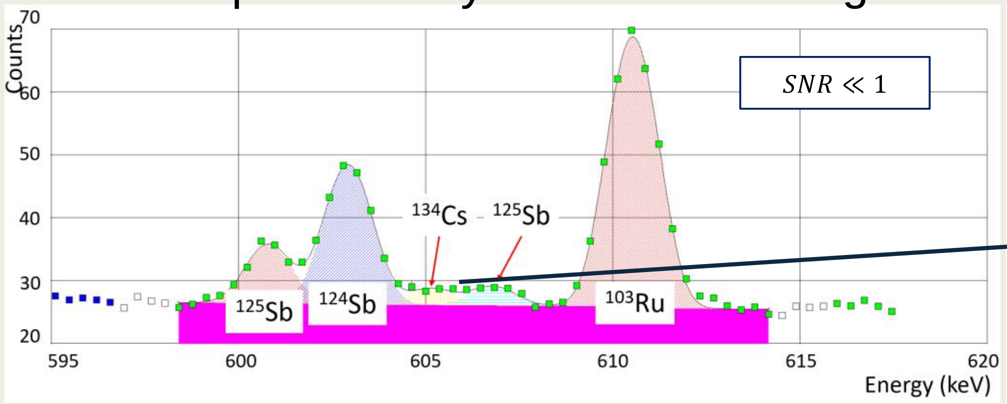

Fig 11. Classic γ-ray with zoom around 605 keV

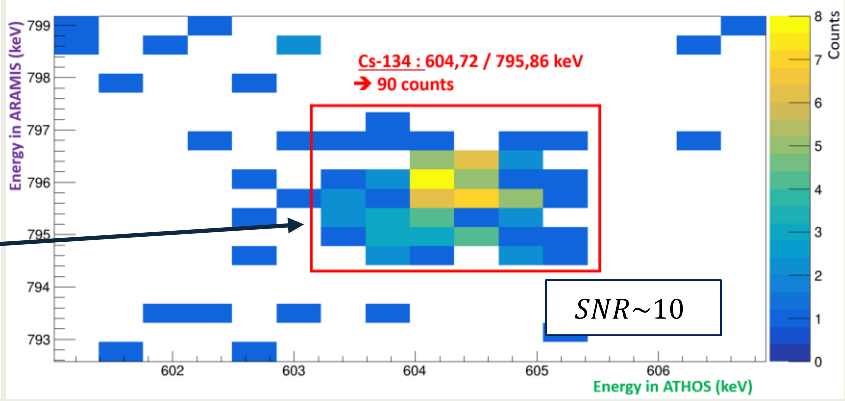

Fig 12. Coincidence matrix with a zoom on the ^{134}Cs

➔ **High SNR values make it easier to qualify and quantify certain radionuclides**

Enhancements of FRL08 : metrological connection between simulation/experimental and utilization of AI tools for coincidence matrix analysis

H.-D. Lenouvel, H. Paradis, A. de Vismes Ott, P. Gross, S. Topin

O3.2-267

Validation of the method on a IAEA sample

- Standard IAEA swipe sample
- Measurement:
  - ATHOS&ARAMIS
  - Duration: 316800 s
- Efficiency calculation:
  - MCNP-CP

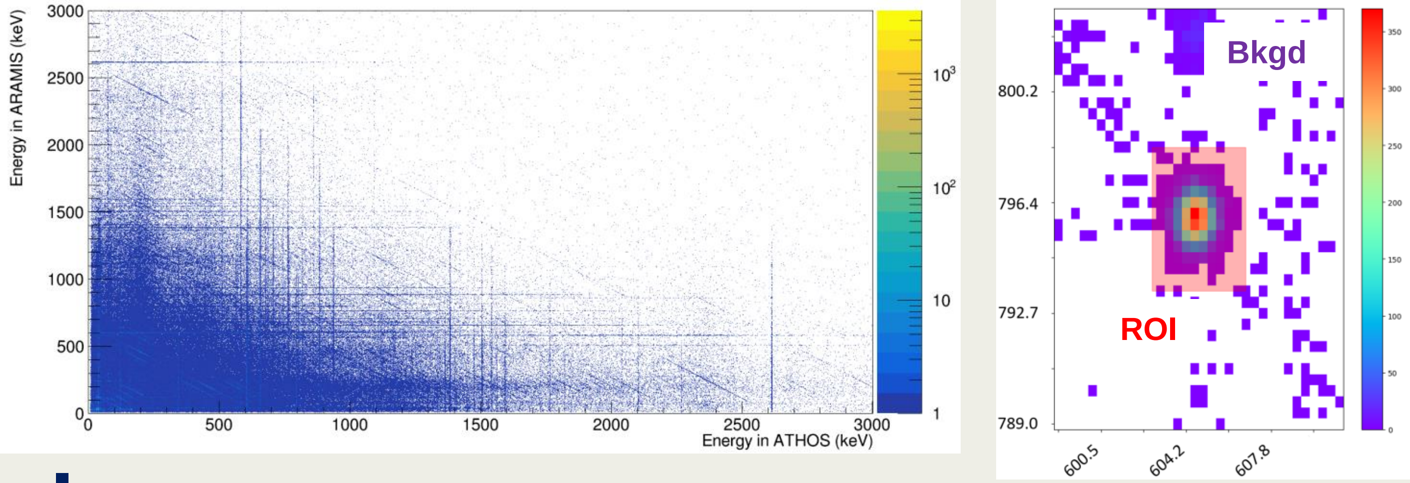

Fig 13. γ/γ **matrix obtained from the measurement with a zoom on the** ^{134}Cs

- Analysis:

Tab 3. Comparison between reference activities and measured activities

Radionuclide	A_{ref} (Bq)	$U(A_{ref})$ k=2 (Bq)	A_{meas} (Bq)	$U(A_{meas})$ k=2 (Bq)	Deviation (%)	E_n score
^{110m}Ag	7.51	0.09	7.36	0.70	-2.0	**-0.21**
^{139}Ce	7.51	0.09	6.7	1.1	-11.0	**-0.78**
^{134}Cs	7.56	0.07	7.75	0.79	2.5	**0.24**
^{152}Eu	7.55	0.07	8.0	0.8	5.7	**0.55**
^{235}U	0.0747	0.0009	0.062	0.027	-16.2	**-0.46**

➔ **Detecting radionuclides (^{134}Cs) with poor visibility in γ-ray spectrometry**
➔ **Validation for γ-ray spectrometry and for γ/γ coincidence spectrometry. Very good agreement with reference values.**

H.-D. Lenouvel, H. Paradis, A. de Vismes Ott, P. Gross, S. Topin

Qualitative AI model

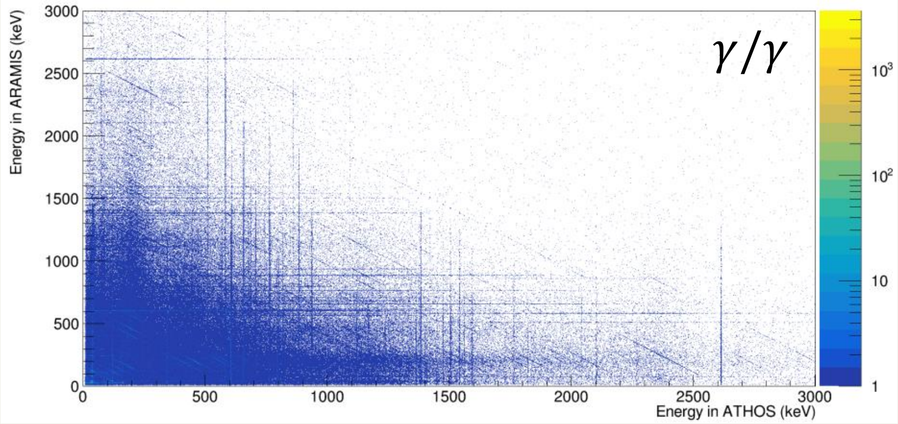

Enhancements of FRL08 : metrological connection between simulation/experimental and utilization of AI tools for coincidence matrix analysis

H.-D. Lenouvel, H. Paradis, A. de Vismes Ott, P. Gross, S. Topin

Database & CNN architecture

- ❑ Memory-intensive 2D spectrum ➔ spectra size reduced by ~300x
- ❑ Composition of simulated samples : ~130 000 spectra
  - ➢ ~3% : spectral signature of each radionuclide of the relevant list
  - ➢ ~18% : fission products from ^{235}U (High Enriched Uranium) with fast neutrons (14 MeV)
  - ➢ ~79% : random distributions

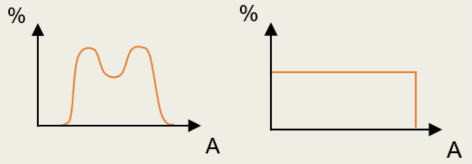

- ❑ Convolutional Neural Network (CNN):

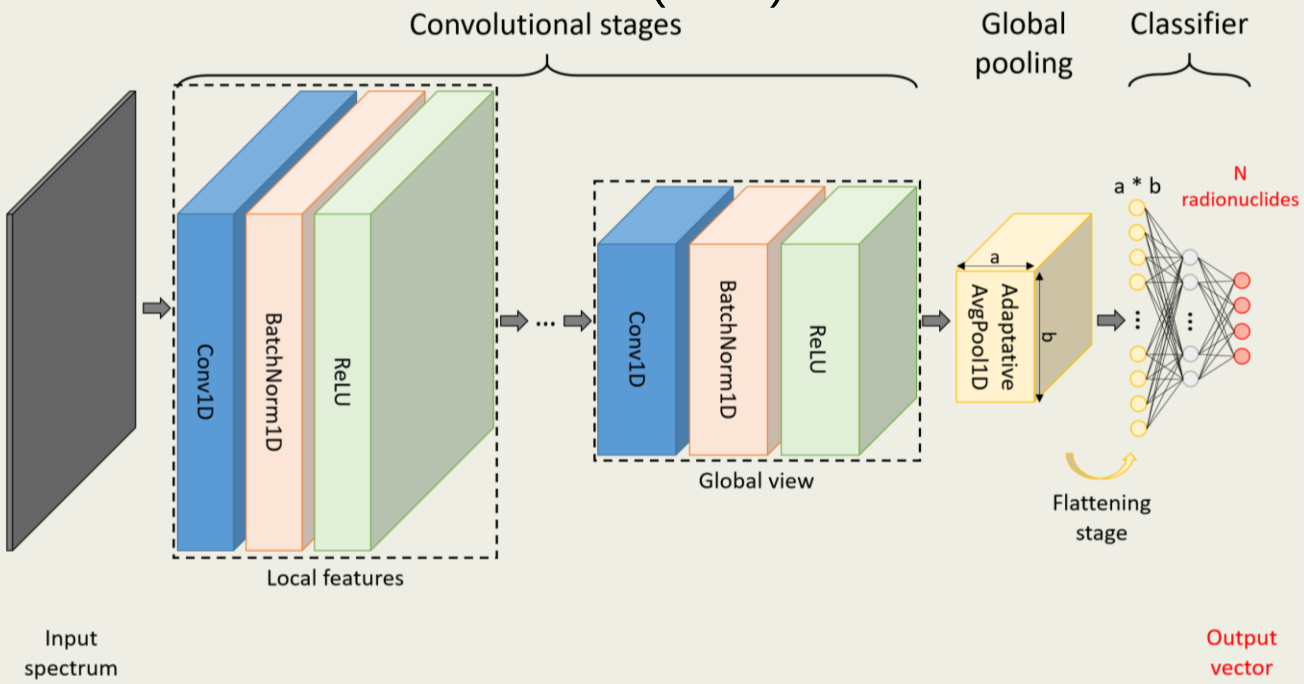

Fig 14. Representation of the CNN architecture employed

➔ **Ensuring both physical accuracy and sufficient representation of each radionuclide**

➔ **Setting thresholds for each radionuclide to determine their presence**

H.-D. Lenouvel, H. Paradis, A. de Vismes Ott, P. Gross, S. Topin

O3.2-267

Evaluation of the spectral CNN

- Determine the model's ability to discriminate between positive and negative classes :

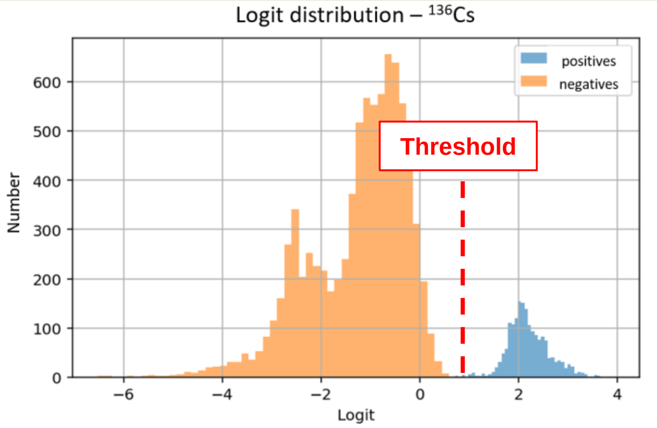

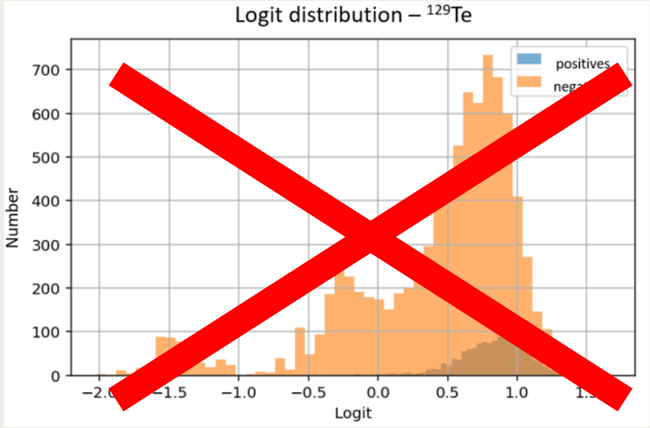

Fig 15. Distribution of positives/negatives as a function of the raw output

- Precision-Recall (PR) curve:

$$Precision = \frac{TP}{TP+FP}$$

$$Recall = \frac{TP}{TP+FN}$$

F1-score (harmonic mean of the precision and recall):

$$F1 = \frac{2*TP}{2*TP+FP+FN} \rightarrow 1$$

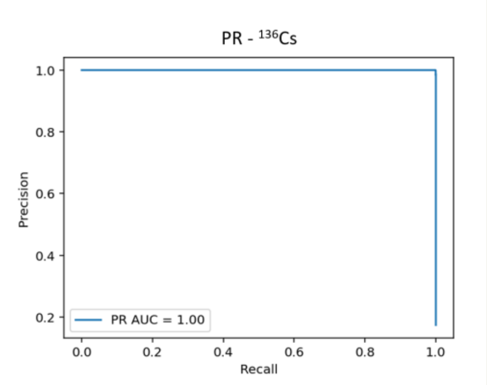

Fig 16. PR curve for ^{136}Cs

For this model:
- Precision: 0.78
- Recall: 0.84
- F1-score: 0.79

➔ **High detection accuracy for specific classes**
➔ **Exclusion of certain classes treated as noise**
➔ **Determine the best threshold**

H.-D. Lenouvel, H. Paradis, A. de Vismes Ott, P. Gross, S. Topin

Results from a standard source

- Radionuclides in the source:
  - Detectable by the model : ^{57}Co, ^{60}Co, ^{88}Y, and ^{139}Ce
  - Undetectable by the model : ^{54}Mn, ^{65}Zn, ^{109}Cd, ^{113}Sn, ^{137}Cs, and ^{241}Am
- CNN results:

Detected
Not detected

Tab 4. Model results on a 10-element standard source

Radionuclide	A (Bq)	Threshold (%)	Predicted probability of presence (%)	Radionuclide	A (Bq)	Threshold (%)	Predicted probability of presence (%)
^{60}Co	185.5	69	85	^{57}Co	105.2	71	24
^{139}Ce	919.5	73	86				
^{88}Y	2794	70	81				

  - ^{57}Co : only visible at low energies

➔ **Most of the elements detectable by the model are correctly classified**
➔ **No false positives were observed**

H.-D. Lenouvel, H. Paradis, A. de Vismes Ott, P. Gross, S. Topin

O3.2-267

Results from the PTE 2023 (3M geometry)

Detected
Not detected

- CNN results:

Tab 5. Model results on a 25-element sample

Radionuclide	Importance	A (Bq)	Threshold (%)	Predicted probability of presence (%)
^{125}Sb	major	2.8	74	78
^{136}Cs	major	21.2	66	82
^{95}Nb	major	26.2	62	85
^{147}Nd	major	35.1	70	74
^{95}Zr	major	63.7	69	96
^{103}Ru	major	81.0	70	98
^{140}Ba	major	93.8	70	93
^{140}La	major	108.0	71	93
^{106}Ru	/	/	68	82
^{124}Sb	major	2.1	68	39
^{156}Eu	minor	3.6	71	43
^{132}Te	minor	7.0	71	16
^{127}Sb	minor	10.2	72	41
^{126}Sb	major	17.5	65	35
^{131}I	major	27.6	69	63
^{134}Cs	/	/	66	19

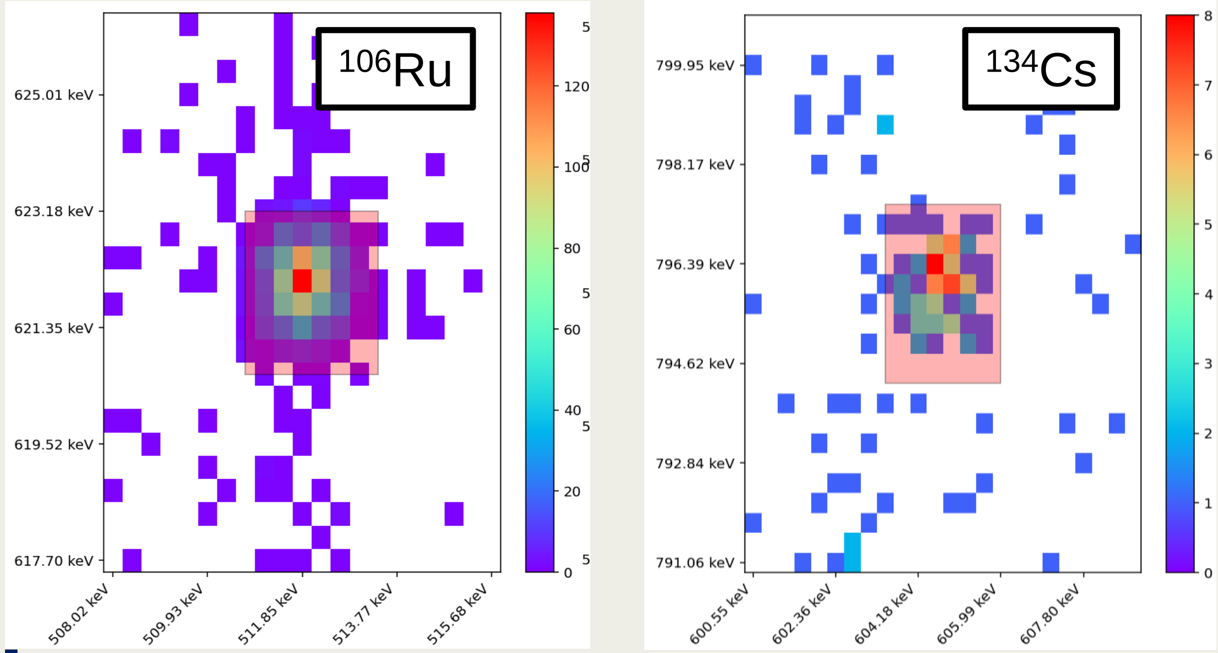

Fig 17. Coincidence matrix with a zoom on the ^{106}Ru and ^{134}Cs

➔ **Most of the elements detectable by the model are correctly classified**

➔ **Most undetected elements are due to low activity/emission levels or insignificant coincidence signatures**

H.-D. Lenouvel, H. Paradis, A. de Vismes Ott, P. Gross, S. Topin

Conclusion & Perspectives

H.-D. Lenouvel, H. Paradis, A. de Vismes Ott, P. Gross, S. Topin

Conclusion

- Metrological connection with Monte Carlo simulation :
  - Model optimization and validation with standard sources
  - Determination of detection efficiencies :
    - Validation with a radioxenon gaseous sample (β/γ coincidence)
    - Validation with IAEA swipe intercomparison exercise (γ/γ coincidence)
- Implementation of a first AI model for γ/γ matrix analysis :
  - Feature detection with a CNN
  - Qualitative multi-label classification

RXe	A_{ref} (Bq)	$U(A_{ref})$ k=2 (Bq)	A_{meas} (Bq)	$U(A_{meas})$ k=2 (Bq)	E_n score
^{131m}Xe	94	10	84	13	-0.60
^{133}Xe	204	23	205	19	0.06
^{133m}Xe	10.2	1.1	9.1	1.4	-0.63
^{135}Xe	217	22	226	21	0.29

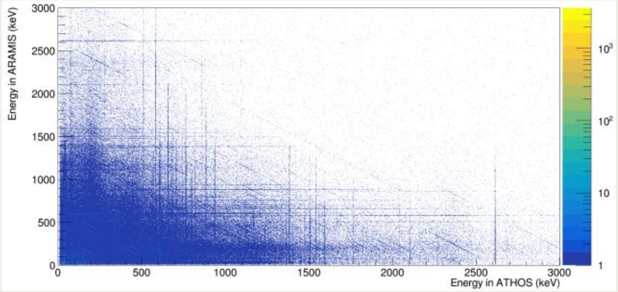

Perspectives

- Optimization of the AI tool:
  - Refine the dataset, improve the network structure and the loss function, for radionuclides whose detection is challenging
  - Include uncertainties to the predicted probabilities of presence
- Explore the use of spectral unmixing method for γ/γ coincidence measurements
  - Adapt the tools developed by **C.-P. Mano (P3.2-263)** to the context of HPGe applications

Thank you.

H.-D. Lenouvel, H. Paradis, A. de Vismes Ott, P. Gross, S. Topin

Annexes

Enhancements of FRL08 : metrological connection between simulation/experimental and utilization of AI tools for coincidence matrix analysis

H.-D. Lenouvel, H. Paradis, A. de Vismes Ott, P. Gross, S. Topin

O3.2-267

Gamma³ : configuration for the measurement of gaseous samples

- Configuration:
  - 2 HPGe: detection of photons (X/γ)
  - 2 PIPS: detection of electrons (e^-/β)
  - The PIPSBox™ is placed between ATHOS and ARAMIS detectors
- β/γ coincidences:

Fig 10. (ATHOS+ARAMIS)&PIPSBox configuration

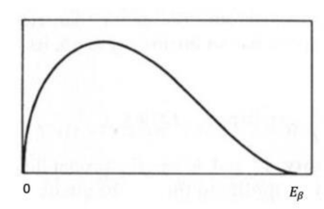

Fig 13. β particle emission energy spectrum

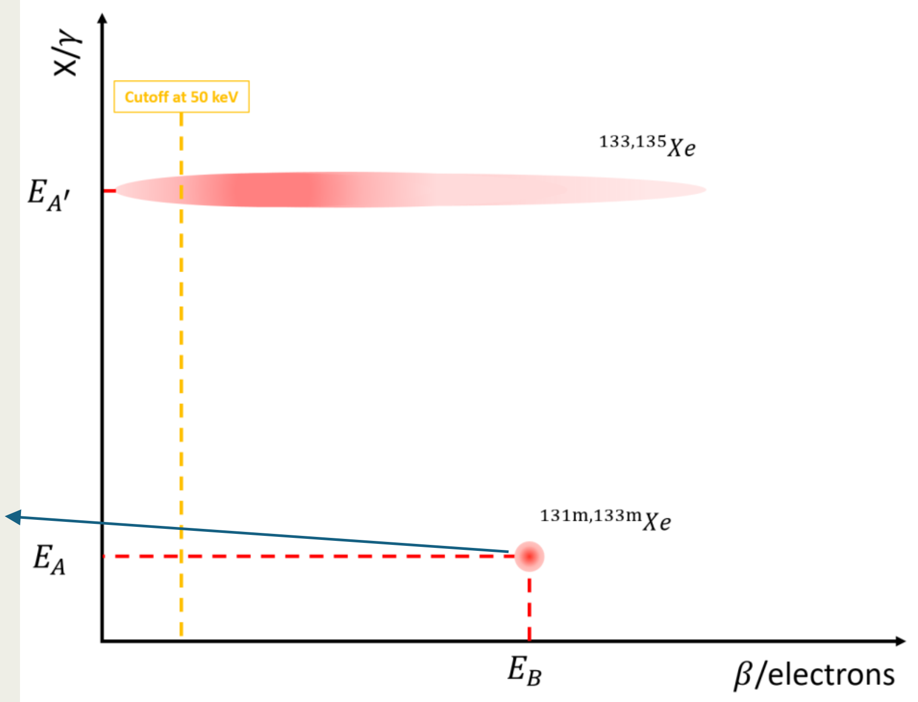

Fig 11. Depiction of the shape of the fingerprints

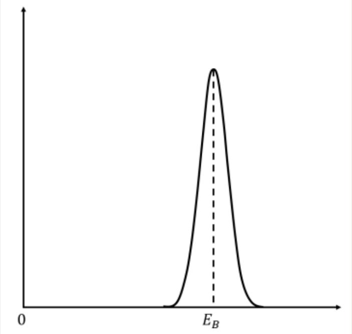

Fig 12. Energy spectrum of the electron emitted by internal conversion

H.-D. Lenouvel, H. Paradis, A. de Vismes Ott, P. Gross, S. Topin

Benefit of using β/γ coincidence detection

- The benefit of using coincidences in the X-ray region:

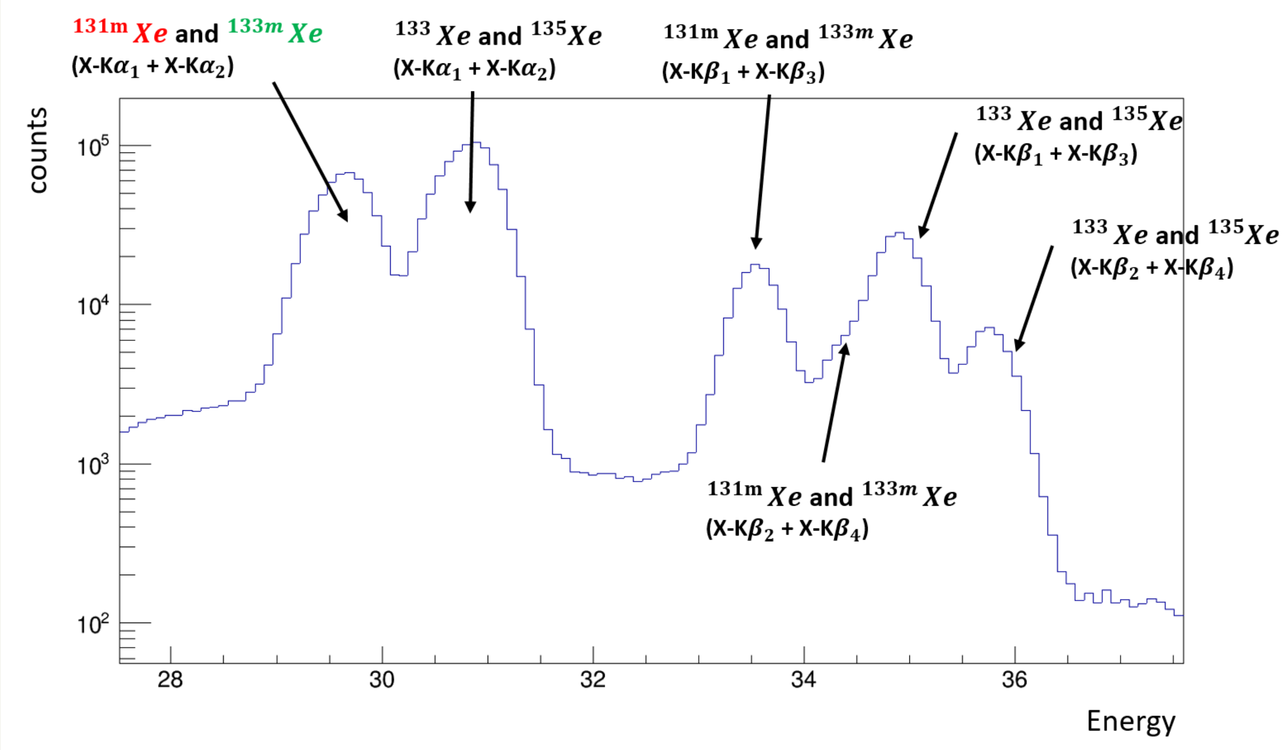

Fig 14. Separation of the signatures of metastable radioxenon isotopes

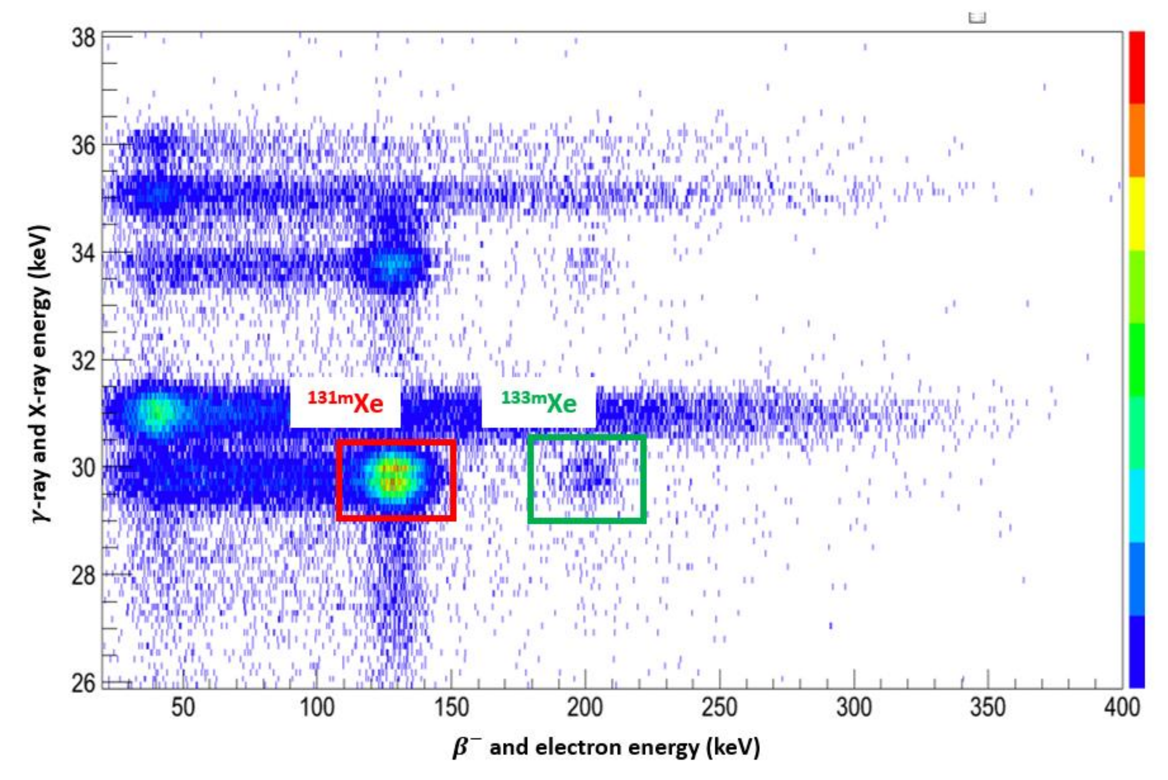

Fig 15. γ-ray spectrum with a zoom on the X-ray region

➔ Characteristic signatures of radionuclide (very low background)

Enhancements of FRL08 : metrological connection between simulation/experimental and utilization of AI tools for coincidence matrix analysis

H.-D. Lenouvel, H. Paradis, A. de Vismes Ott, P. Gross, S. Topin

O3.2-267

- Calculation of decision thresholds (D_T) and detection limits (D_L) on a blank measurement:
  - ISO standard 11929
  - Comparison between the classical and coincidence spectrometry

- Particulate radionuclides:

Radionuclide	γ spectrometry : D_T / D_L (mBq)	γ/γ spectrometry : D_T / D_L (mBq)
^{108m}Ag	2.03 / 4.2	0.39 / 2.9
^{110m}Ag	2.44 / 5.0	3.67 / 26.4
^{60}Co	1.81 / 3.8	0.60 / 4.3
^{125}Sb	5.31 / 10.9	5.39 / 19.0
^{134}Cs	1.75 / 3.6	0.71 / 3.2

Tab 6. Comparison of D_T/D_L between γ and γ/γ spectrometry for particulate measurements

➔ Regarding certain radionuclides : $P * \varepsilon$ very low ➔ $LD_{\gamma\gamma} > LD_\gamma$

➔ $SD_{\gamma\gamma}$ often highly favorable➔ better sample characterization

- Noble gas sample:

Radionuclide	γ spectrometry : D_L (mBq)	β/γ spectrometry : D_L (mBq)
^{131m}Xe	73	0.3
^{133}Xe	3.3	1.0
^{133m}Xe	33	0.2
^{135}Xe	18.3	4.3

Tab 7. Comparison of D_T/D_L between γ and β/γ spectrometry for noble gas measurements

➔ β/γ spectrometry highly favorable for metastable radioxenon isotopes

H.-D. Lenouvel, H. Paradis, A. de Vismes Ott, P. Gross, S. Topin

Training of the spectral CNN

- Activation function : sigmoid

  ➔ raw outputs → probabilities of presence

  - multi-labels classification

- Loss function : Custom FocalLoss [5] with BCEWithLogit

  ➔ $FL(p_t) = -\alpha_t(1-p_t)^{\gamma} * BCEWithLogits$

  - α → balances positive vs. negative classes
  - γ → focuses on hard vs. easy examples

- Optimizer : Adam (step : 10^{-5})

Here :
- Epochs : 15
- Batch : 128 spectra
- $\alpha = 0.9$ / $\gamma = 2.5$

➔ **Strong class imbalance + avoiding underfitting of difficult classes**

[5] T.-Y. Lin et al., Facebook AI Research (FAIR), 2017